Optical Review
https://doi.org/10.1007/s10043-019-00575-7

REGULAR PAPER

Optical design for transfer of camera viewpoint using retrotransmissive optical system

Naoya Koizumi[1,3] · **Yudai Niwa**[2] · **Hajime Kajita**[2] · **Takeshi Naemura**[2]

Received: 23 May 2019 / Accepted: 24 December 2019

Abstract
We propose a virtual camera that can pass through a small hole in an obstruction to capture an image on the other side. Recently, free-viewpoint television technology has enabled the generation of video in which viewpoint images are captured from locations where cameras are not actually placed. However, capturing the images of objects concealed behind obstructions or beyond a camera's field of view is a challenge. We designed an optical transformation system that utilizes a conventional camera, concave lens, and transmissive mirror device (TMD); this system enables the capture of images through small holes in walls or other obstructions. Our experimental prototype demonstrated that it is possible to capture images of the area on the other side of a wall through a 5 mm hole. In this paper, modulation transfer function (MTF) comparison is used to show that a combination of a concave lens and TMD is an effective optical design for a midair camera.

Keywords Midair imaging · Camera · Viewpoint · Retrotransmissive optical system

1 Introduction

Computational photography has enabled cameras to exceed the limitations of those that use the conventional method [1]. This research field has enabled the creation of images that include additional attributes such as images with all objects in full focus, images with depth, images with a high dynamic range, images with gigapixel resolution, images in full wavelength, and images taken from a viewpoint around a corner. With such novel camera capabilities, images that could not have been obtained before are now possible. However, it is difficult to capture an image if the target objects are hidden from the camera's view. One approach to solving this problem is non-line-of-sight (NLOS) imaging, which reconstructs the shape and albedo of hidden objects using multiple scattered lights [2]. However, it is difficult to capture color data. A color sensor similar to that of a camera is required to capture color data, but if there is a small hole in a physical barrier such as a wall, it is difficult to see what is on the other side of the wall even if the camera is brought close to the hole. If it is possible to position a virtual camera at the hole, as shown in Fig. 1, we can capture what is on the other side of the wall while maintaining a wide angle of view of the camera θ_{camera} as shown in Fig. 1. If the camera captures images from the edge of the hole, its angle of view is only θ_{shoot}. However, if the viewpoint of the virtual camera can be placed inside the hole, as shown in Fig. 1 (right), images with a wide angle of view can be taken.

In this paper, we propose an optical system that can work as a virtual camera positioned inside a small hole in a wall. In this study, we designed an optical transformation system by combining a camera and an optical system comprising a concave lens and a transmissive mirror device (TMD). Using this system, people can capture images from locations where obstacles prevent them from entering or where they cannot physically place a camera.

2 Related work

In this study, we apply midair image optical systems to the design of a virtual camera. There are several techniques for forming midair images such as reflecting a light source to

✉ Naoya Koizumi
koizumi.naoya@uec.ac.jp

1 University of Electro-Communications, 506, Building W-3, 1-5-1 Chofugaoka, Chofu, Tokyo 182-8585, Japan

2 University of Tokyo, 7-3-1 Hongo, Bunkyo, Tokyo 113-8656, Japan

3 JST, PRESTO, Saitama, Japan

Published online: 10 January 2020

Fig. 1 Conventional camera (left) and our camera (right)

form an image in the air. FLOATS V [3] and FuwaVision [4] are available as techniques using Fresnel lenses. Recently, another midair imaging technology using a reflective material consisting of special structures instead of a lens has been proposed. Aerial imaging by retroreflection (AIRR) [5] is another way to form a midair image with a wide viewing angle using cost-effective and robust optical components. It uses three elements: a light source, half mirror, and retroreflector. Light emitted from the light source is reflected by the half mirror and propagates to the retroreflector, and then the retroreflected light is transmitted through the half mirror and converges at the midair image position, which is the plane-symmetrical position of the light source with respect to the half mirror. This is a very effective way to form a midair image, but the attenuation of brightness is a problem. A roof mirror array (RMA) [6] and retroreflective mirror array [7] are also mirror-based optical devices that form midair images. However, they are not commercially available.

On the other hand, a transmissive mirror device (TMD) is already commercially available and is easier to handle than a conventional nonlinear optical system. Light incident to the TMD is reflected twice in a mirror and converges at a position that is plane-symmetric to the TMD. Since the TMD does not have a fixed focal length, the imaging position can easily be moved by changing the distance between the light source and the TMD without changing the size of the resulting image. There are several TMDs such as aerial imaging plates (AIPs) [8], DCRA [9, 10], CMA [11], and parallel RMA [12]. As we describe below, we choose an AIP in this study because it is the largest available TMD and is easy to install.

3 Design

The purpose of this study is to place a virtual camera in a certain location in the air. It is assumed that the viewpoint can be moved and placed in a small hole in a wall to look on the other side of the wall.

There are three design requirements: the optical axis condition (AXIS), linearity (LINEARITY) and the depth of field condition (FOCUS). AXIS ensures that there is no image distortion due to the optical axis. LINEARITY ensures that there is linearity between the moving distance of the physical camera and the midair camera viewpoint. For example, if a physical camera is moved 10 cm in a certain direction, the virtual camera viewpoint will move 10 cm in the corresponding direction. FOCUS ensures that the depth of field can be adjusted. The photographic optical system developed in this study satisfies all three requirements, as shown in Table 1. The key concept is to use a TMD to optically transfer camera functions. However, if there is only a TMD and camera, the focus direction of the virtual camera is reversed and becomes opposite to that of the target. Thus, we fix a concave lens to the camera to change the focus direction. Fig. 2 shows a diagram of the key concept, which we describe in detail in the following subsection.

3.1 Optical transfer by lens

First, we describe the structure, features, and problems of a single-lens system with one convex lens and a two-lens afocal system.

The single-lens system is the most basic system for moving a camera viewpoint toward a convex lens element surface. A problem of this method is image distortion occurring when the camera deviates from the optical axis. Therefore, the control range of the camera is restricted by the optical axis of the lens.

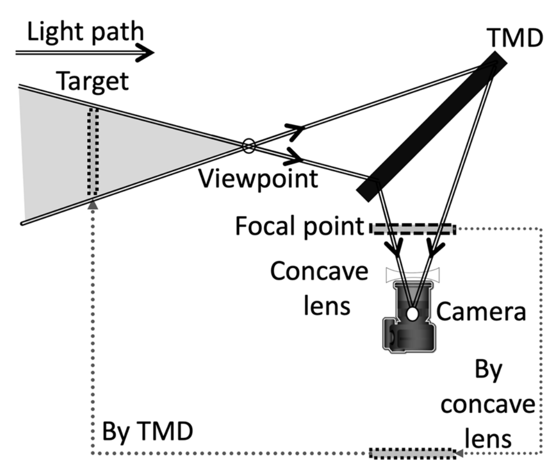

Fig. 2 Key concept of our method. A TMD and concave lens are combined to form a virtual camera

Table 1 Requirements of midair camera

	AXIS	LINEARITY	FOCUS
Single lens			✓
Afocal optics		✓	✓
Our goal	✓	✓	✓

In an afocal optical system, two convex lenses are separated by the distance equal to the sum of their focal lengths and the optical axes are aligned. A feature of this system is linearity in the positional relationship before and after transfer in a certain range. However, an optical axis also exists in the afocal system. Therefore, similar to the single-lens system, when the control range of the camera deviates from the optical axis of the afocal system, image distortion occurs.

3.2 Optical transfer by transmissive mirror device

As we describe below, the optical axis of the lens causes image distortion. In this study, we use a TMD, which has no optical axis when combined with a camera.

An advantage of the TMD is that the image is distortion free owing to the optical axis of the lens and the linearity of the positional relationship between the source and the image. Regarding the former, since the TMD is an optical system with no optical axis, the distortion caused by the optical axis of the lens can be suppressed. Therefore, in contrast to a single-lens system and an afocal system, it is possible to control the camera three-dimensionally and apply it to a multicamera system. Regarding the latter, the TMD is an optical system that reimages light rays from a light source at plane symmetrical positions with respect to it. Therefore, since the camera viewpoint is transferred from the camera to the plane symmetrical position with respect to the TMD, the positional relationship is linear.

The problem of the combination of a TMD and camera is that the target cannot be focused on. Since the TMD forms an image at a symmetrical position, the depth direction is reversed. Assuming that the target side is forward with respect to the camera viewpoint position, the transferred virtual camera faces in the direction opposite to the forward direction. Therefore, the focus position is also reversed, and the image obtained without focusing on the target is blurred. Additionally, if the aperture is narrowed and a pinhole camera is used, an all-focus image can be obtained, but it is too dark to be used as an optical sensor. Thus, this combination does not meet the specifications required for a system with an adjustable depth of field.

3.3 Combination of the TMD and lens

In this study, we design a method of eliminating the inversion of the direction of focus while using the transfer of the viewpoint of the camera provided by the retroreflective optical system. The reason why the camera image is not in focus is that the focus position is transferred to the side opposite to the target because the front-to-rear relationship on the imaging side caused by the TMD is switched. Therefore, we compare a method of inverting the viewpoint direction of the camera by combining two TMDs and a method of transferring only the position of the camera focus by combining a convex lens or a concave lens with TMDs. In the comparison, we consider whether the following two methods satisfy the required specifications.

– Brightness: higher brightness is better.
– Unobstructed: no part of the system overlaps the transferred camera viewpoint.

If we use TMDs, there are two feasible combinations: one using two TMDs and one using combination of a TMD and lens. In the method using two TMDs, since the inversion of the front-to-rear relationship of the camera viewpoint position and the focus position occurs twice, the camera body returns to the front-to-rear relationship. An advantage of this method is that the camera viewpoint can pass through small gaps because no physical object is required at the virtual camera viewpoint. On the other hand, the disadvantage of this method is the darkness and large size of the system. When light passes through two TMDs, the amount of light entering the camera is reduced by about 25%. The second method combines a TMD, convex lens, and camera as shown in Fig. 3. The camera faces the TMD, which is tilted 45° in the horizontal direction, and the convex lens is placed in the camera viewpoint position transferred by the TMD. The camera focal plane is transferred to the subject side as a virtual focal plane via the TMD, and then the convex lens transfers the virtual focal plane to the target position. In this way, the camera can focus on the target without decreasing the brightness. If the transmittance by the glass lens is 80%, the light entering the camera through the convex lens is reduced to 40%. This is considered to be 1.6 times brighter than the 25% reduction when using two AIPs. In this case, if the camera position changes, it is necessary to move the convex lens to the corresponding camera viewpoint position, which complicates the system.

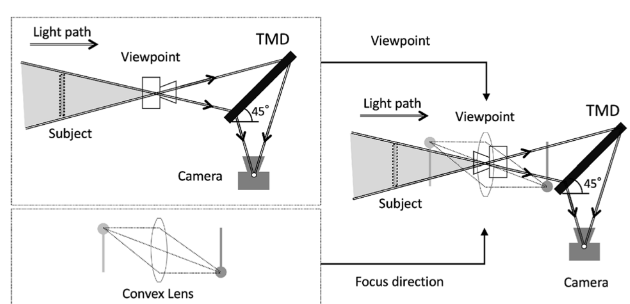

Fig. 3 Combination of TMD and convex lens

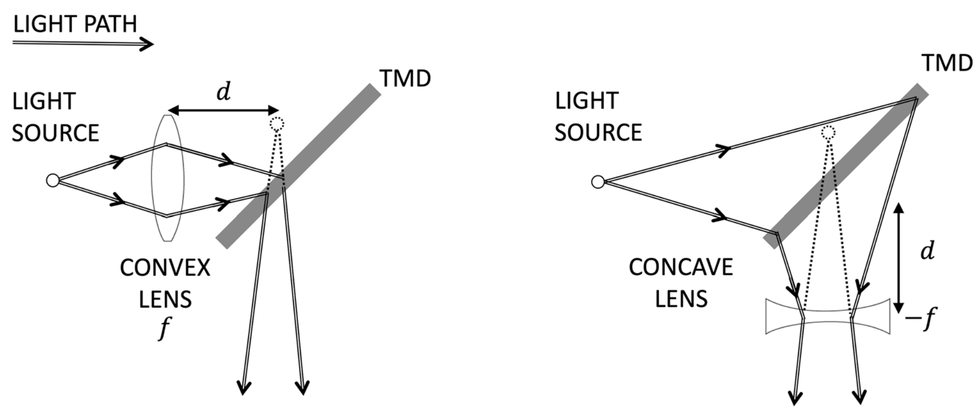

Fig. 4 Convex–concave conversion by TMD

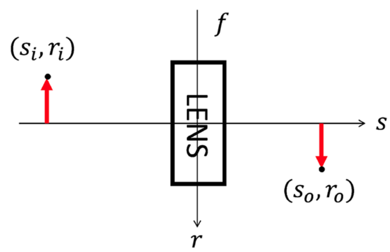

Fig. 5 Coordinate conversion by lens

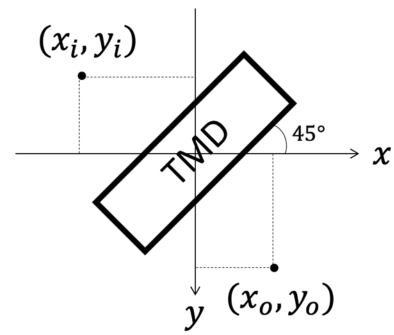

Fig. 6 Coordinate conversion by TMD

3.4 Convex–concave conversion

Here we show that an optical system in which a convex lens and TMD are placed in this order and an optical system in which a concave lens is placed at a position symmetrical to the convex lens with respect to the TMD are optically equivalent, where optically equivalent means that if the input is the same, the output is the same regardless of the behavior of the light beam. This is called convex–concave conversion by the TMD. Fig. 4 shows an illustration of convex–concave conversion.

As shown in Fig. 5, a lens having focal length f placed at the origin with the s axis as the optical axis converts the coordinates of a point light source existing at a certain position (s_i, r_i) to (s_o, r_o). From the lens formula, the following relationship holds for s_i, s_o, and f.

$$\frac{1}{s_o} = \frac{1}{s_i} + \frac{1}{f}$$

This formula is solved for s_o as follows.

$$s_o = \frac{f}{s_i + f} s_i$$

Therefore, the output coordinates (s_o, r_o) can be expressed by the following formula.

$$(s_o, r_o) = \frac{f}{s_i + f}(s_i, r_i)$$

Furthermore, if the lens position is moved in parallel by distance d, it can be transformed as follows.

$$(s_o - d, r_o) = \frac{f}{s_i - d + f}(s_i - d, r_i)$$
$$(s_o, r_o) = \frac{f}{s_i - d + f}(s_i - d, r_i) + (d, 0)$$

A TMD converts a point light source to a symmetrical position with respect to the TMD. As shown in Fig. 6, the TMD is inclined 45° from the x axis and placed at the origin. The output coordinates (x_o, y_o) of the input (x_i, y_i) are given by

$$(x_o, y_o) = (-y_i, -x_i).$$

Fig. 7 shows an optical system that combines a TMD placed at the origin and a convex lens with focal length f_1 placed at $x = d_1$. Furthermore, the figure shows an optical system combining a TMD placed at the origin and a lens having focal length f_2 placed at $y = d_2$. Here we find the conditions that make these two optical systems equivalent.

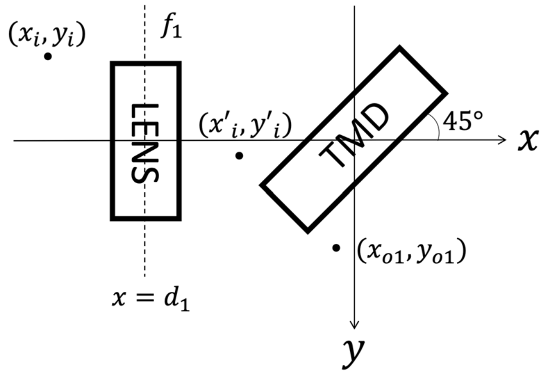

Fig. 7 Coordinate conversion by convex lens and TMD

When the coordinates of the light are converted from (x_i, y_i) to (x_{o1}, y_{o1}) via (x_i', y_i') by a convex lens and TMD, the input coordinates (x_i, y_i) and output coordinates (x_{o1}, y_{o1}) can be expressed as follows.

$$\begin{aligned}(x_{o1}, y_{o1}) &= (-y_i, -x_i) \\ &= -(y_i, x_i) \\ &= -\left(\frac{f_1}{x_i + f_1 - d_1}(y_i, x_i - d_1) + (0, d_1)\right) \\ &= \frac{-f_1}{x_i + f_1 - d_1}(y_i, x_i - d_1) + (0, -d_1)\end{aligned}$$

Next, Fig. 8 shows an optical system that combines a TMD and a concave lens. When the coordinates of light are converted from (x_i, y_i) to (x_{o2}, y_{o2}) by the concave lens and TMD, the input coordinates (x_i, y_i) and output coordinates (x_{o2}, y_{o2}) can be expressed by the following equation.

$$(x_{o2}, y_{o2}) = \frac{f_2}{x_i - f_2 + d_2}(y_i, x_i + d_2) + (0, d_2)$$

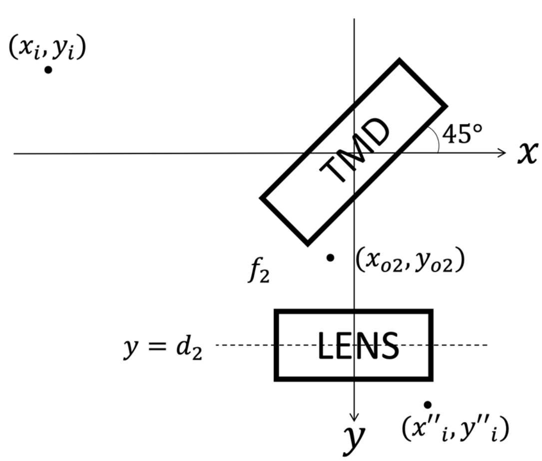

Fig. 8 Coordinate conversion by concave lens and TMD

The conditions required for $(x_{o1}, y_{o1}) = (x_{o2}, y_{o2})$ to be satisfied for any (x_i, y_i) are obtained as follows from this equation.

$$d_1 = -d_2 \tag{1}$$

$$f_1 = -f_2 \tag{2}$$

Therefore, it has been shown that the optical systems shown in Figs. 7 and 8 are equivalent. As a result, a convex lens placed on the subject side can be replaced by a concave lens on the imaging side. This is convex–concave conversion.

3.5 Proposed design

Our proposed design is a combination of a TMD, concave lens, and camera. The concave lens is directly attached to the camera so that the optical axis of the camera and that of the concave lens coincide. The camera focal plane is transferred to the symmetrical position of the subject with respect to the TMD using the concave lens, and then the TMD transfers the virtual focal plane to the subject position. During this time, the movement of the concave lens and that of the camera are unified because these two components are fixed.

Table 2 shows the additional requirements of the three optical designs. We found that the combination of a TMD and a concave lens is useful as it provides the brightest image and has the simplest design.

4 Implementation

To design and implement the midair camera, it is necessary to set the focus range and perspective. Figure 9 shows the transfer of the focus position by the TMD and convex lens. We assume that the x and y axes are independent axes, and the focus position on the y axis is transferred to the x axis by AIP. The origin of the x and y axes is the center of the TMD, and the camera and convex lens are placed at the position of $-L$ on the x and y axes, respectively. The focal length of the convex lens is assumed to be f.

Table 2 Additional requirements of optical designs as below for mid-air camera

	Brightness	Unobstructed
TMD + TMD	×	✓
TMD + convex lens	✓	×
TMD + concave lens	✓	✓

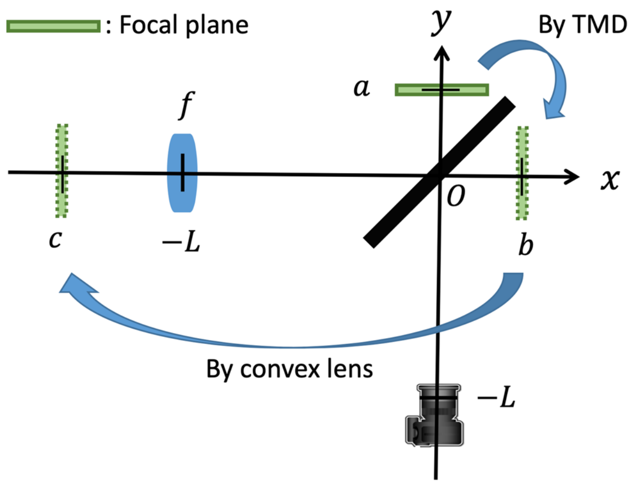

Fig. 9 Transformation of focal plane

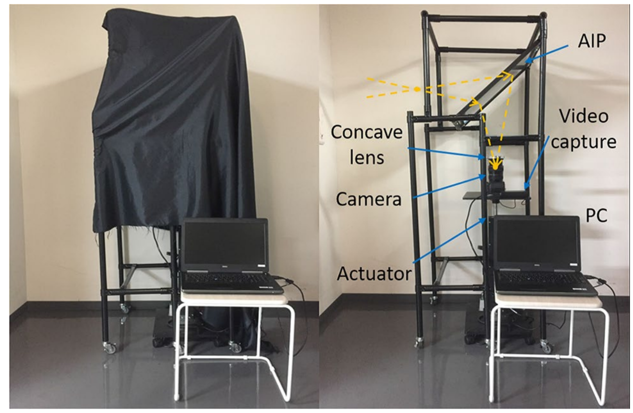

Fig. 10 Experimental setup

4.1 Lens spec for focus transfer

First, we describe the focus range. Captured images blur when a camera and TMD are combined because the focus direction of the camera is reversed by the TMD. Suppose that the focus of $y = a$ from the camera placed at $y = -L$ is transferred to $x = b$ on the x axis by the TMD, and finally transferred to $x = -c$ by the convex lens. Here, the relationship between a and b is obtained from the TMD feature.

$$a = b$$

Furthermore, starting from the lens formula, the following relationship is established between the focal lengths f, b, and c.

$$\begin{aligned}
\frac{1}{f} &= \frac{1}{c-L} + \frac{1}{b+L} \\
\frac{1}{f} &= \frac{(b+L)+(c-L)}{(c-L)(b+L)} \\
\frac{1}{f} &= \frac{b+c}{(c-L)(b+L)} \\
f &= \frac{(c-L)(b+L)}{b+c} \\
fb + fc &= cb + cL - bL - L^2 \\
fc - cb - cL &= -L^2 - bL - bf \\
c(f-b-L) &= -L^2 - bL - bf \\
c &= -\frac{L^2 + bL + bf}{(f-b-L)}
\end{aligned}$$

c is length $c > 0$ must be satisfied. That is, $f - b - L < 0$ must be satisfied. Therefore, $a = b < f - L$, and a must be controlled so that it exceeds the focal length f of the lens.

4.2 Perspective

Next, we describe the perspective. In this study, the concave lens is fixed on the camera lens with their optical axes aligned. If the focal length of the camera is f_{cam}, the focal length of the concave lens is $f_{concave}$, and the distance between these two lenses is l_{lens}, the combined focal length f_{modify} can be expressed as follows.

$$f_{modify} = \frac{f_{concave} f_{cam}}{f_{concave} + f_{cam} - l_{lens}} \tag{3}$$

Furthermore, the angle of view θ_{view} can be obtained from the focal length (f_{modify}) and the size of the CMOS image sensor (l_{sensor}) as follows.

$$\theta_{view} = 2\tan^{-1}\left(\frac{l_{sensor}}{2f_{modify}}\right) \tag{4}$$

The above formula requires that the TMD is within the angle of view as seen from the camera. Therefore, when the TMD size is constant, the angle of view becomes narrower when the camera body and TMD are separated. In addition, the experiment described later is performed with the optical axis fixed so that it is not displaced, and we did not examine how much the deviation of optical axis affects the perspective and image quality.

4.3 Prototype

Figure 10 shows the experimental setup used to demonstrate the proposed system. We used an AIP as the TMD. The dimensions of the AIP were 488 mm × 488 mm × 4 mm (W × D × H), the pitch interval was 0.5 mm, and the AIP was fixed to metal pipes. A camera (main unit, Canon EOS 5D Mark II; lens, EF24—105 mm F4L IS USM) equipped with a concave lens (Clear Optical Co., Ltd., RQ-04, 90 mm) was placed on an actuator facing the AIP, which was directly above the camera. This system made it possible to move the camera viewpoint back and forth by raising and lowering a linear actuator. If the viewpoint of the camera is placed at the position of a small gap, the camera can capture images behind it. To minimize the effect of ambient light, the upper side of this system was surrounded with a dark curtain. The image captured by the camera was output to a laptop (Dell Precision 7520, Windows 10) via video capture (MonsterX U 3.0 R).

5 Evaluation

To confirm the effectiveness of our design, we measured the MTF under five conditions by the edge method. A target was photographed close-up from a midair position. By comparing the measured values, we demonstrated two advantages of our design: the capability to adjust the depth of field and the high sharpness of the images obtained.

5.1 Experimental conditions

As a prerequisite for this measurement, it was assumed that close-up images were taken from the position where the camera protrudes as far as possible from the AIP. Thus, we placed the viewpoint as far as possible from the AIP and fixed the focus position to be as close to the camera as possible. The distance between the AIP and the camera was fixed at 40 cm. This was to maximize the range of use of the AIP when the angle of view is fixed at the minimum (maximum zoom). The distance from the camera viewpoint to the edge of the subject was set to 13 cm, which is the shortest shooting distance in the proposed method. Thus, the distance from the AIP to the edge was fixed at 53 cm. Also, to display the edge image as the target, we used an iPad 2 (Apple Inc.) as a light source with constant brightness. This is an IPS-type LCD tablet with a size of 9.7 inches and 1024 × 768 pixels. We measured the brightness of the light source with a luminance meter (CS-100A). The brightnesses of white and black were 352 cd/m^2 and 0.5 cd/m^2, respectively, so the contrast ratio was 704:1. Among the five conditions used to measure the MTF, three conditions are a combination of the AIP and camera, and the second condition corresponds to the proposed method. The combination of the AIP and camera is hereinafter referred to as AIP + camera.

Table 3 shows the details of the five conditions and Fig. 11 shows an overview thereof. The conditions are classified according to three elements: the system (AIP + camera or proposed method), aperture (OPEN or CLOSED), and the focus position (INFINITY or MACRO) of the camera body. Regarding the aperture setting, OPEN was set to the maximum value when opened (F value: 4.0), and CLOSED was set to the most closed case (F value: 22.0). Moreover, we adjusted the ISO value via the aperture value (400 for OPEN and 6400 for CLOSED) to compensate for the change in brightness of the image owing to changes in the aperture. With regard to the focus position, the relationship between the AIP and the camera is reversed by the transfer, and the perspective relationship is switched in the proposed method. In particular, with regard to AIP + camera, when the focus position of the camera body is set to INFINITY, the focus position of the camera body is transferred by the AIP from the camera viewpoint to INFINITY on the side opposite to the target (AIP side).

To calculate the MTF, we used the images taken by the experiment setup. After photographing the edge image, it was converted to grayscale. Then, to minimize the effect of the parts other than the edge, we clipped the edge part of the image and calculated the pixel value. In this measurement, the central portion of the image was used to minimize the effect of the aberration of the concave lens.

5.2 Evaluation

Four points were confirmed by carrying out comparisons described in the following bulleted list. The comparisons were carried out in the low-frequency region because of the lower effect of noise in this region.

– Is it possible to express bokeh in the proposed design?

  1. Expression of bokeh by proposed optical system: system (d) or system (e)

– Is sharpness improved by adding a concave lens?

  2. Improved resolving power by attaching a concave lens: system (a) or system (e)

Table 3 Experimental conditions

	System	Aperture	Focus of camera body	Focus of midair camera
(a)	AIP + camera	OPEN	INFINITY	Invese INFINITY
(b)	AIP + camera	CLOSE	INFINITY	Inverse INFINITY
(c)	AIP + camera	CLOSE	MACRO	Inverse INFINITY
(d)	Proposed method	OPEN	MACRO	INFINITY
(e)	Proposed method	OPEN	INFINITY	MACRO

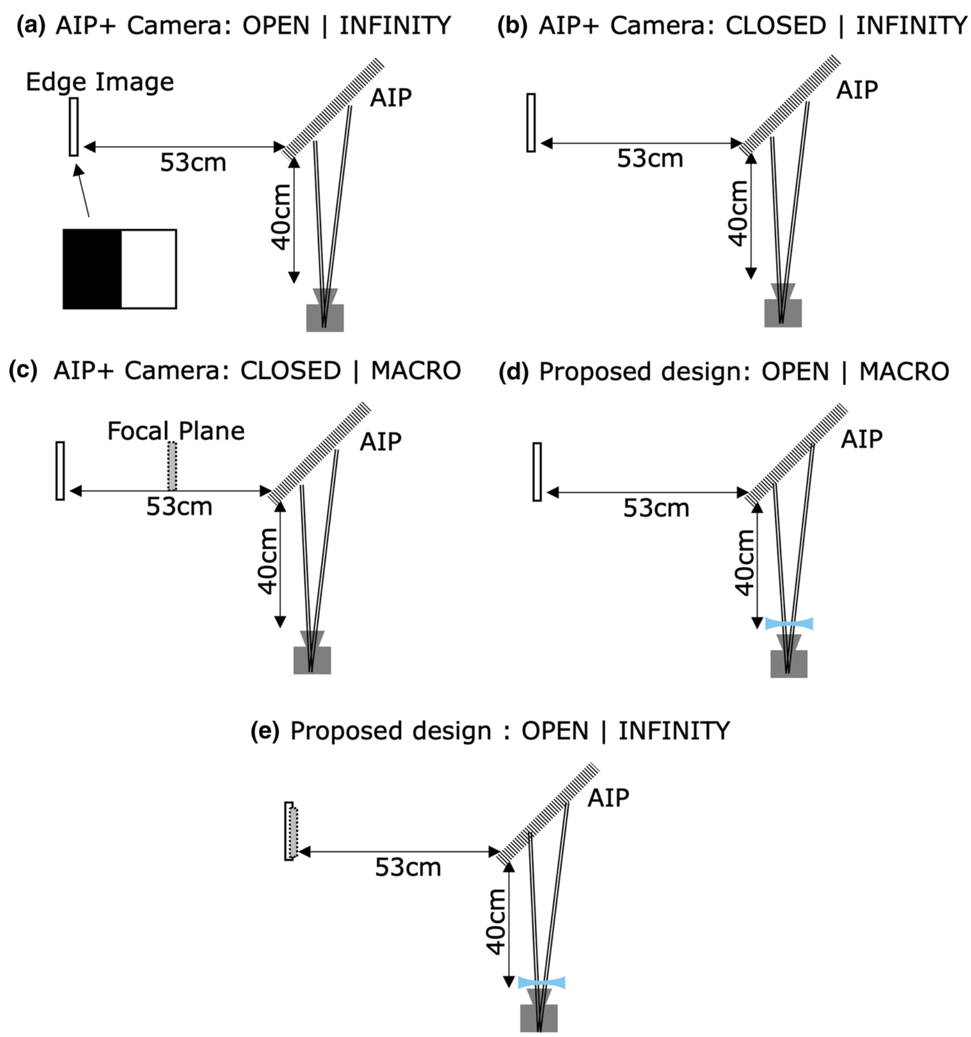

Fig. 11 Experiment setup. There are five conditions whose settings are given in Table 3. The distance between the edge image and the AIP is 53 cm and the distance between the camera and the AIP is 40 cm

3. Comparison of sharpness of systems combining the AIP and camera: system (b) or system (c)
4. Comparison of sharpness of the proposed optical system and the AIP + camera system; the better of system (b) and (c) (comparison 3) is compared with system (e).

In comparison 1, the only difference between (d) and (e) is the focus position. Therefore, if it is possible to control the depth of field, it will be out of focus in (d) and in focus in (e). In other words, it is confirmed that the depth of field changes.

The difference between comparison 1 and comparison 2 is the presence or absence of a concave lens. Therefore, the effect of attaching the concave lens can be measured.

In comparison 3, we determine the condition with the highest sharpness with AIP + camera. In systems (b) and (c), the target position is not in the focal plane. Therefore, it is predicted that the smaller the aperture, the better the result. For comparison 4, we compared the proposed design with AIP + camera.

5.3 Results

The MTFs up to 1.5 LP/mm under all conditions are shown in Fig. 12, and captured edge images are shown in Fig. 13.

We shall examine the adjustment of the depth of field under comparison 1. It can be seen that there is a difference in sharpness for the focused system (e) and the defocused system (d); therefore, it is possible to adjust the depth of field by our proposed design. Also, we will consider the change in sharpness owing to the addition of a concave lens under comparison 2. By comparing system (a) and system (e), we found that the MTF of system (e) is always higher than that of system (a) when the resolving power is under 1.5 LP/mm. System (a) has a lower MTF than system (e) at 0.2 LP/mm or more. Therefore, it can be concluded that the improvement in sharpness is due to the placing of the

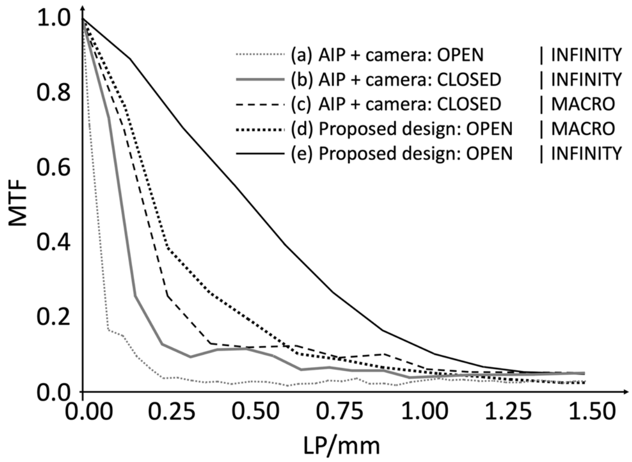

Fig. 12 MTFs under five conditions

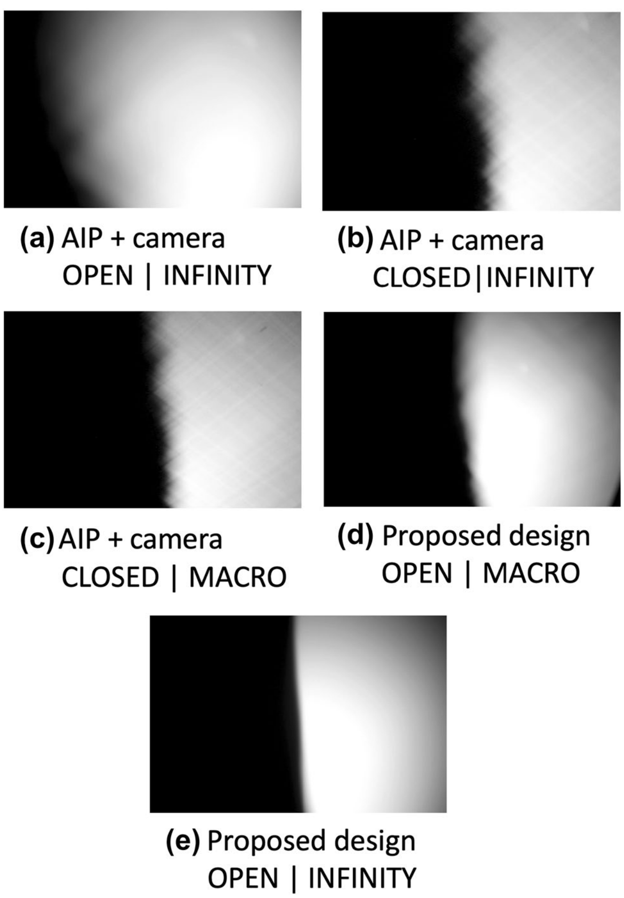

Fig. 13 Edge images under five conditions

concave lens. Next, the combination of the AIP and camera was compared according to comparison 3. The MTF of system (c) is better than that of system (b). Therefore, when realizing a midair camera with a combination of an AIP and camera, it is best to close the aperture of the camera so that the aperture is similar to that of a pinhole camera.

From comparison 3, it is found that system (c) has the optimum resolution when the AIP and camera are combined. Therefore, systems (c) and (e) are compared. The resolving power is higher under system (e) up to around 1.3 LP/mm, which is almost equal to the resolving power above 1.3 LP/mm.

6 Applications

With this design, it is possible to capture images through gaps in debris in disaster sites or through animal cages without disturbing the natural behavior of the animal. We confirmed the limit in the hole size through a heuristic experiment involving holes in paper using our prototype. Figure 14 shows the setup of this experiment. We used a camera (Sony α 7R II) with a normal lens (Sony SEL2470GM; focal length, 24–70 mm) and concave lens (KENIS; H-7; focal length, −250 mm). When the aperture was opened to its maximum, it was possible to capture images of the area through a 5 mm hole. The experiment was conducted in a room where a fluorescent lamp was lit, and the ambient illumination was 709 lx. Figure 14a shows the device and obstacles seen from the side. During the actual experiment, the entire device was covered with a black cloth so that light from outside did not enter. Figure 14b shows an obstacle with a 5 mm square hole.

Figure 15a shows the experimental setup as seen from behind. The image obtained when a person is in front of the hole is shown in Fig. 15b. The distance between the hole and the person is 130 cm. The ISO is set to 3200, F is 4, and the exposure time is 1/60. Figure 15c, d show the situation and image obtained when a person is sitting to the side of the front desk, respectively.

In this experimental setup, the measured angle of view was about 66.1° when viewed from the front. This is different from the theoretical value given in Sect. 4.2. The reason for

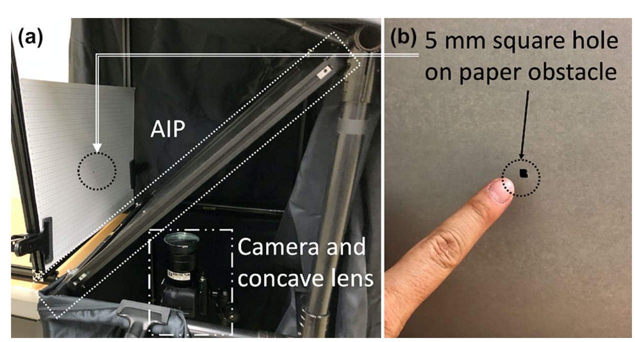

Fig. 14 Setup for experiment on capturing images through hole

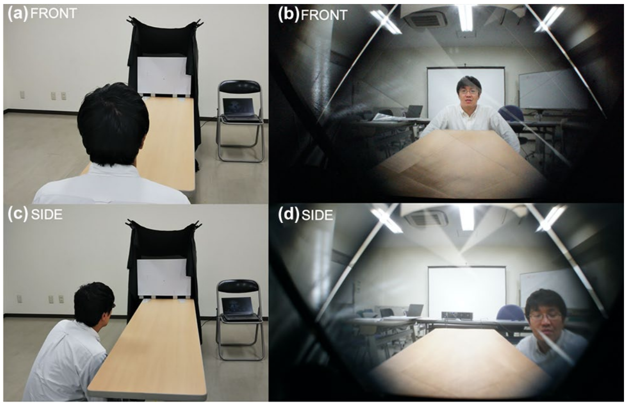

Fig. 15 Setup for experiment on capturing image through hole

the difference is that there are places where stray light from the AIP enters and cannot be photographed.

The current limitations of this method are thought to be due to this behavior of the stray light. In the future, we will research on the acquisition of images from multidirectional viewpoints using stray light or the removal of stray light by considering polarization.

7 Conclusion

In this paper, we realized a system that works as a midair camera that can be positioned at a small hole while maintaining a wide angle of view. This makes it possible to take more natural photographs of people and animals because the target is not aware of the camera when capturing images from a position with the camera protruding from the camera body. It was mathematically demonstrated that using an optical system that combines a convex lens with a camera, one way capture images from a position where the photographing viewpoint is outside the main camera body, but the problem of image distortion caused by the optical axis occurs. Therefore, we proposed a photographing system combining a transmissive optical system with no optical axis and a camera. Owing to the specifications of the transmissive optical system, there was a problem that the anteroposterior relationship of the focus position was reversed, making it impossible to focus the camera. However, by attaching a concave lens to the camera, one can adjust the depth of field. From the results of experiments, it was confirmed that the depth of field can be adjusted and the sharpness can be improved by adding a concave lens. Furthermore, we confirmed that it is possible to capture images from a position where the camera viewpoint was outside the camera body, and this was demonstrated using the proposed system.

Acknowledgements This research was supported in part by a Grant in aid for Precursory Research for Embryonic Science and Technology (PRESTO) and CREST from the Japan Science and Technology Agency (JPMJPR16D5).

References

1. Nayar, S.K.: Computational cameras: redefining the image. Computer **39**(8), 30–38 (2006)
2. O'Toole, M., Lindell, D.B., Wetzstein, G.: Real-time non-line-of-sight imaging. In: ACM SIGGRAPH 2018 Emerging Technologies, SIGGRAPH '18, vol. 14, pp. 1–14:2, ACM, New York (2018)
3. Kakeya, H.: P-65: FLOATS V: real-image-based autostereoscopic display with TFT-LC filter. SID Symp. Dig. Tech. Pap. **35**(1), 490–493 (2004)
4. Nii, H., Zhu, K., Yoshikawa, H., Htat, N.L., Aigner, R., Nakatsu, R.: Fuwa-Vision: an auto-stereoscopic floating-image display. In: SIGGRAPH Asia 2012 Emerging Technologies, SA '12, vol. 13, pp. 1–13:4, ACM, New York (2012)
5. Yamamoto, H., Tomiyama, Y., Suyama, S.: Floating aerial LED signage based on aerial imaging by retro-reflection (AIRR). Opt. Express **22**(22), 26919–26924 (2014)
6. Maeda, Y., Miyazaki, D., Maekawa, S.: Volumetric aerial three-dimensional display based on heterogeneous imaging and image plane scanning. Appl. Opt. **54**(13), 4109–4115 (2015)
7. Koike, T., Onishi, Y.: Aerial 3D imaging by retroreflective mirror array. In: Companion proceedings of the 2018 ACM international conference on interactive surfaces and spaces, ISS '18 Companion, pp. 25–29, ACM, New York (2018)
8. Otsubo, M.: Optical imaging apparatus and optical imaging method using the same, US8702252B2 (2014)
9. Maekawa, S., Nitta, K., Matoba, O.: Transmissive optical imaging device with micromirror array. In: Three-dimensional TV, video, and display V, vol. 6392, pp. 130–137. International Society for Optics and Photonics, SPIE (2006)
10. Yoshimizu, Y., Iwase, E.: Radially arranged dihedral corner reflector array for wide viewing angle of floating image without virtual image. Opt. Express **27**(2), 918–927 (2019)
11. Yamamoto, H., Bando, H., Kujime, R., Suyama, S.: Design of crossed-mirror array to form floating 3D LED signs. In: Stereoscopic displays and applications XXIII, vol. 8288, pp. 705–712. International Society for Optics and Photonics, SPIE (2012)
12. Maeda, Y., Miyazaki, D., Maekawa, S.: Optical design for heterogeneous imaging based on retro reflection using parallel roof mirror arrays. In: JSAP-OSA Joint Symposia 2014 Abstracts, pp. 20a_C4_3. Optical Society of America (2014)